View metadata, citation and similar papers at core.ac.uk
brought to you by CORE
provided by Elsevier - Publisher Connector

Amyloid β-peptide polymerization studied using fluorescence correlation spectroscopy

Lars O Tjernberg[1], Aladdin Pramanik[2], Sofie Björling[2], Per Thyberg[2], Johan Thyberg[3], Christer Nordstedt[1], Kurt D Berndt[2], Lars Terenius[1] and Rudolf Rigler[2]

Background: The accumulation of fibrillar deposits of amyloid β-peptide (Aβ) in brain parenchyma and cerebromeningeal blood vessels is a key step in the pathogenesis of Alzheimer's disease. In this report, polymerization of Aβ was studied using fluorescence correlation spectroscopy (FCS), a technique capable of detecting small molecules and large aggregates simultaneously in solution.

Results: The polymerization of Aβ dissolved in Tris-buffered saline, pH 7.4, occurred above a critical concentration of 50 μM and proceeded from monomers/dimers into two discrete populations of large aggregates, without any detectable amount of oligomers. The aggregation showed very high cooperativity and reached a maximum after 40 min, followed by an increase in the amount of monomers/dimers and a decrease in the size of the large aggregates. Electron micrographs of samples prepared at the time for maximum aggregation showed a mixture of an amorphous network and short diffuse fibrils, whereas only mature amyloid fibrils were detected after one day of incubation. The aggregation was reduced when Aβ was incubated in the presence of Aβ ligands, oligopeptides previously shown to inhibit fibril formation, and aggregates were partly dissociated after the addition of the ligands.

Conclusions: The polymerization of Aβ is a highly cooperative process in which the formation of very large aggregates precedes the formation of fibrils. The entire process can be inhibited and, at least in early stages, partly reversed by Aβ ligands.

Addresses: [1]Laboratory of Biochemistry and Molecular Pharmacology, Section of Drug Dependence Research, Department of Clinical Neuroscience, the Karolinska Hospital, S-171 76 Stockholm, Sweden. [2]Department of Medical Biochemistry and Biophysics, [3]Department of Cell and Molecular Biology, Medical Nobel Institute, the Karolinska Institute, S-171 77 Stockholm, Sweden.

Correspondence: Lars Tjernberg (amyloid β-peptide) or Rudolf Rigler (fluorescence correlation spectroscopy)
E-mail: Lars.Tjernberg@cmm.ki.se or Rudolf.Rigler@mbb.ki.se

Key words: Alzheimer's disease, amyloid β-peptide, fluorescence correlation spectroscopy, polymerization

Received: **20 April 1998**
Revisions requested: **21 May 1998**
Revisions received: **30 October 1998**
Accepted: **5 November 1998**

Published: **22 December 1998**

Chemistry & Biology January 1999, **6**:53–62
http://biomednet.com/elecref/1074552100600053

© Current Biology Ltd ISSN 1074-5521

Introduction

Deposition of amyloid β-peptide (Aβ) fibrils in brain parenchyma and vasculature is an invariable feature of Alzheimer's disease [1–3]. There is substantial evidence that the formation of these fibrillar deposits is a central event in the disease pathology. For instance, all known mutations that segregate with familial Alzheimer's disease lead to increased production of $A\beta^{1-42}$ and deposition of amyloid plaques early in life [4–9]. Transgenic mice expressing these mutated genes show neuropathological lesions similar to those found in Alzheimer's disease [10,11], and Aβ has been shown to become toxic to cells upon polymerization [12–14]. Consequently, the nature of the polymerization process and its potential inhibition are relevant topics to study, and small molecules capable of binding to Aβ are potential drugs for the prevention and treatment of the disease [13,15–19].

The polymerization process has been studied *in vitro* using different techniques, including turbidimetry [20–23], light scattering [23–28], analytical ultracentrifugation [20], circular dichroism spectroscopy (CD) [29–31], electron microscopy (EM) [32], atomic force microscopy [33–35], polyacrylamide gel electrophoresis (PAGE) [29,36,37], size-exclusion chromatography (SEC) [25,38] and quantitative fluorimetry [32,39]. Only the spectroscopic techniques are able to measure the polymerization process directly in solution. So far, quasielastic light scattering has provided the most detailed description of this process [27,28]. In order to follow the polymerization of Aβ in solution we used fluorescence correlation spectroscopy (FCS). In FCS, the fluorescence of single dye-labeled molecules excited by a sharply focused laser beam is observed. From the intensity fluctuations, which are due to varying numbers of molecules in the volume element of observation, the average number of molecules can be obtained directly using an intensity correlation function. Components with different molecular weights and correspondingly different diffusion times can be analyzed using FCS without prior separation [40–45]. The high sensitivity of FCS, which allows analysis in the nanomolar range and below, opens up various new possibilities in the analysis of molecular interactions. In this paper, FCS was used to follow the polymer-

ization of Aβ in solution, observing monomers/dimers and aggregates of different sizes simultaneously. FCS was also applied to investigate how the presence of Aβ ligands affects the polymerization process. The ligands used were peptides capable of binding to the Lys–Leu–Val–Phe–Phe ($Aβ^{16–20}$) sequence, previously shown to be critical for Aβ Aβ binding and fibril formation [18,19]. Part of these results were reported previously in a thesis [46].

Results

FCS studies of Aβ polymerization using rhodamine-labeled Aβ as fluorescent probe

In the first set of experiments, the polymerization of $Aβ^{1–40}$ in Tris-buffered saline (TBS), pH 7.4, was studied with rhodamine-labeled Aβ as fluorescent probe. From the fluorescence intensity fluctuations of free rhodamine and of rhodamine-labeled $Aβ^{1–40}$, the diffusion times ($τ_D$) were calculated using the autocorrelation function and found to be 40 μs and 90 μs, respectively. When compared with rhodamine (443 Da), which was used as a reference, the diffusion time of labeled Aβ corresponded to a molecular weight of about 5 kDa (theoretical value 4870 Da), assuming diffusion of spherical particles. There was no evidence to suggest that aggregates were present at the start of incubation. It has been shown that Aβ rapidly forms dimers in solution [28,38] and it is possible that the population of molecules observed in the freshly prepared solutions represents a mixture of monomers and dimers. Within the first 2 min after dissolution of $Aβ^{1–40}$ (80 μM), no change in diffusion time was observed (Figure 1a–c), indicating that no aggregation occurred during this period. After 10 min plenty of large aggregates were detected and after 40 min the aggregation reached a maximum (Figures 1d–f and 2). After 40 min of incubation, the fluorescence intensity fluctuations exhibited several peaks with highly increased heights (Figure 1d). These peaks, with up to three times higher intensity than the baseline level, clearly represent Brownian motion of Aβ aggregates containing several rhodamine-labeled Aβ molecules. The diffusion time for these aggregates was found to be 3 s (Figure 1e). Similar diffusion times were obtained when the intensity autocorrelation functions (Figure 1b,e) were analyzed using the CONTIN algorithm [47,48] (Figure 1c,f). After 80 min of incubation the diffusion time of the aggregates had changed from 3 s to 0.3 s. No further changes in diffusion time and the amount of aggregates were detected between 2 h and 24 h (data not shown). From the diffusion times of around 0.3 s and 3 s, the hydrodynamic radii of equivalent spheres (Equation 5; see the Materials and methods section) were calculated to be 6 μm and 60 μm, respectively. For the 0.3 s species, the length of a rigid rod with a diameter of 100 nm (corresponding to the diameter of the fibril bundles detected using electron microscopy, EM, Figure 3c) was calculated to be 55 μm (Equation 7; see the Materials and methods section).

Electron microscopy

Samples were prepared for EM after incubating solutions of Aβ for 1 min, 40 min or 1 day. No material was detected after 1 min of incubation, but after 40 min an amorphous network and short fibrils could be seen (Figure 3a,b). Mature fibrils, but no amorphous network or short fibrils, were shown to be present in the sample incubated for 1 day (Figure 3c). The fibrils were often arranged in bundles, about 100 nm wide and 5–20 μm long, or in an irregular network. Without centrifugation preceding the EM analysis, only a few fibrils were detected, indicating that fibrils remained in solution and did not sediment to any major extent at 1 × g. When 80 μM $Aβ^{1–40}$ was incubated in the presence of 320 μM LBMP1620 (a peptide capable of binding to Aβ; see below), only a few occasional fibril bundles could be detected by EM, which instead revealed small amorphous aggregates (not shown).

The influence of concentration on Aβ polymerization

$Aβ^{1–40}$ was dissolved directly in 50 mM Tris–HCl and 150 mM NaCl (TBS) at concentrations ranging from 1 μM to 300 μM. The aggregation was strongly dependent on concentration and the critical concentration for rapid polymerization was found to be 50 μM (Figure 4). Below this concentration only monomers/dimers were detected. Above this concentration the polymerization to large aggregates proceeded rapidly after a lag phase of a few minutes.

Quantification of peptides in supernatants using high performance liquid chromatography

Aliquots of 5 μl were aspirated from the upper half of the FCS samples and 15 μl formic acid was added (in order to dissolve aggregates) prior to injection into the reverse-phase column. The samples containing up to 100 μM Aβ showed no significant decrease in Aβ concentration,

Figure 1

The polymerization of Aβ studied by FCS using rhodamine-labeled Aβ as fluorescent probe. Aβ (80 μM) was incubated with rhodamine-labeled Aβ (10 nM). The fluorescence intensity fluctuations (due to rhodamine-labeled Aβ molecules diffusing through the volume element of observation) were measured after **(a)** 2 min and **(d)** 40 min. The corresponding intensity autocorrelation functions, G(τ), were calculated using Equation 1. The observed and calculated data points are completely overlapping. Their difference is shown as residuals underneath (Figure 1b,e). **(b)** The monophasic form of the curve indicates that the diffusion times for the different species present are similar. The diffusion time, $τ_D$, was found to be 90 μs. **(e)** After 40 min of incubation, the calculated autocorrelation function has a biphasic appearance. Species with a very high diffusion time ($τ_D$ = 3 s), corresponding to very large aggregates, as well as the initial monomers/dimers ($τ_D$ = 90 μs) can be observed. **(c,f)** The distribution of diffusion times, $P(τ_D)$ was calculated from the autocorrelation function using the CONTIN algorithm (Equation 3). Note that only few, if any, intermediate-sized aggregates were present.

indicating that the decrease in large aggregates in those samples not was due to precipitation. Samples with over 100 μM Aβ and samples with ligand concentrations over 320 μM showed a decline in peptide concentration over time (data not shown).

The effect of Aβ ligands on polymerization

The experiments were repeated in the presence of peptides capable of binding to Aβ (and blocking its aggregation); LBMP1620, Lys–Leu–Val–Phe–Phe, Asn–Lys–Leu–Val–Phe–Phe–Ala, and leu–phe–leu–arg–arg (all D-amino

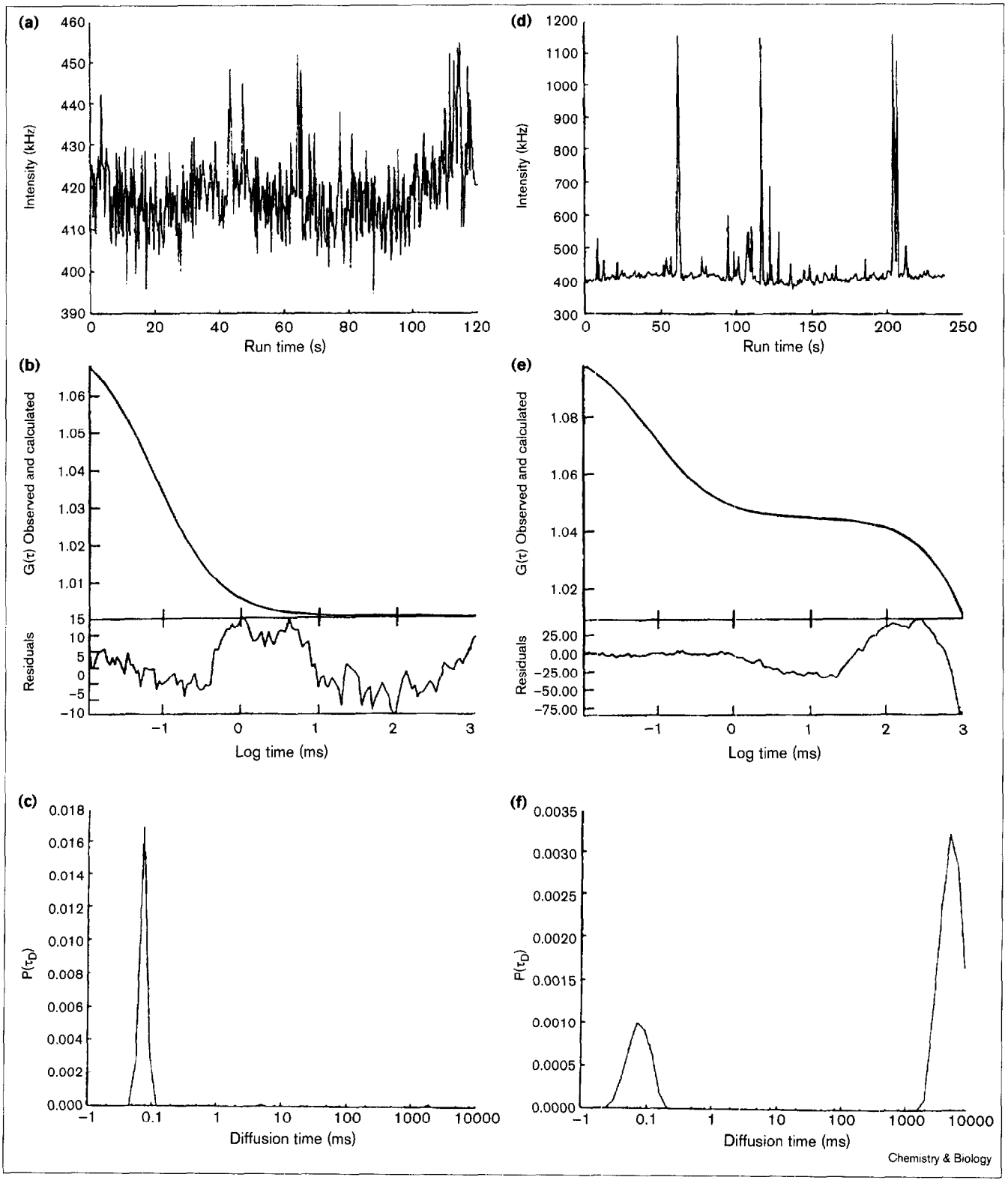

Figure 2

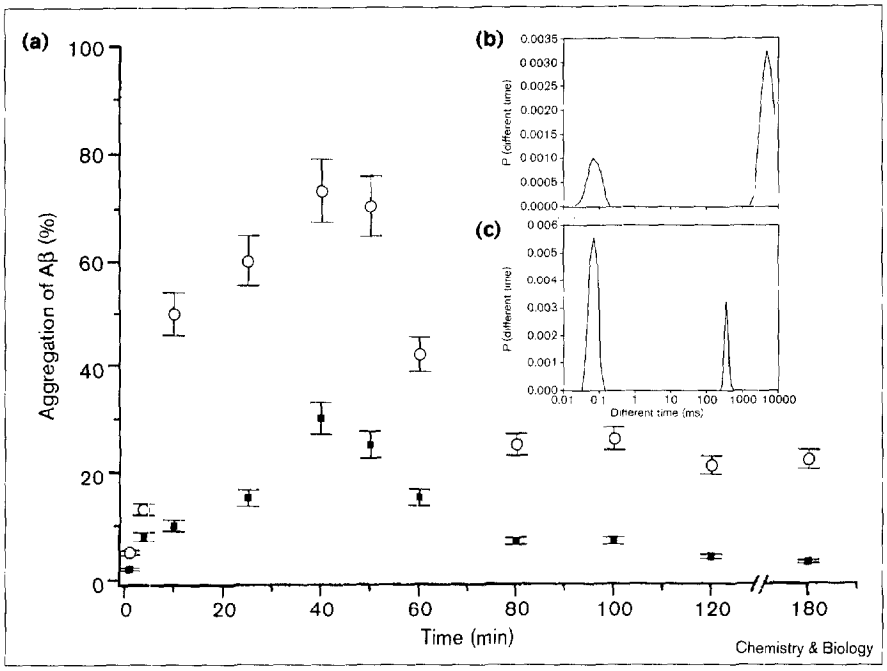

Time course of Aβ polymerization. Aβ (80 μM) was incubated with rhodamine-labeled Aβ (10 nM) and the intensity fluctuations were measured at several time points ranging from 2 min to 24 h. The diffusion times and the percentage of Aβ aggregates were calculated by Equations 1 and 2. **(a)** The relative amount of aggregates was plotted as a function of incubation time (open circles). The effect of the Aβ-binding heptapeptide LBMP1620 on polymerization was studied by incubating 80 μM Aβ and 10 nM rhodamine-labeled Aβ in the presence of 320 μM LBMP1620 (filled squares). Distribution of diffusion times of Aβ aggregates after **(b)** 40 min and **(c)** 120 min incubation.

acids), and the nonbinding peptide Lys–Ala–Leu–Val–Phe–Phe–Ala. The heptapeptide LBMP1620 was found to inhibit aggregation most efficiently. A significantly lower amount of aggregates was formed in the presence of ligand. The effect of LBMP1620 on aggregation over time is shown in Figure 2. After 3 h of incubation the amount of aggregates was 20–25% in the absence of ligand (Figure 5b), and 3–4% in the presence of ligand (Figure 5d). Some of the aggregates, with diffusion times in the range of 1–20 ms, were not observed in the absence of ligand. The nonbinding peptide Lys–Ala–Leu–Val–Phe–Phe–Ala had no effect on the aggregation of Aβ (data not shown). When LBMP1620 was dissolved at a concentration of 320 μM in a solution containing aggregated Aβ (80 μM Aβ, aged for 1 h), a depolymerization process was initiated. The monomer/dimer concentration was ~95% after 2 h of additional incubation, with a concomitant disappearance of large aggregates (Figure 5c).

FCS studies of Aβ polymerization using labeled ligand as fluorescent probe

To investigate the binding characteristics of the $A\beta^{16-20}$ sequence, labeled ligand (rhodamine-Lys–Lys–Leu–Val–Phe–Phe) was used as fluorescent probe in one set of experiments. The diffusion time for labeled ligand dissolved in TBS, pH 7.4, was found to be 60 μs, which corresponds to a molecular weight of 1.5 kDa (theoretical molecular weight = 1298 Da). As for Aβ, therefore, the ligand can exist as a mixture of monomers and dimers. When labeled ligand was incubated in the presence of 1 mM LBMP1620, no change in diffusion time was detected (data not shown). When solutions containing Aβ (100 μM) were incubated in the presence of labeled ligand, large aggregates were observed. The diffusion times of these aggregates were found to be the same as those detected with labeled Aβ (Figure 5a,e). When LBMP1620 was dissolved at 400 μM in an aggregated solution of 100 μM Aβ (aged for 1 h), the diffusion time changed from 3 s to 0.1 ms, and no aggregates (τ_D = 3 s) were observed after incubation with the ligand (Figure 5f). When labeled $A\beta^{1-40}$ was used, aggregates could still be observed after the addition of an excess of LBMP 1620 (Figure 5c). This difference (compare Figure 5c with 5f) indicates that the labeled ligand is displaced by LBMP 1620.

Circular dichroism spectroscopy

In order to further characterize the starting material and to follow possible changes in Aβ conformation during the formation of the large aggregates detected with FCS, CD analysis was performed. CD spectra taken at 20 and 80 μM Aβ, which corresponds to concentrations below and above the cooperative transition as observed by FCS (Figure 4), were similar, both showed typical disordered conformation (random coil; Figure 6a). Also, under conditions that show the time-dependent aggregation process by FCS (Figure 2), no changes occurred in the CD spectrum during incubation between 2 min and 24 h (Figure 6b, inset). Even in this case, the CD spectrum is of random- coil type. CD spectra are recorded in the same buffer as used in FCS experiments (TBS). For comparison, spectra are also recorded in phosphate buffer, which allows the CD spectra to be analysed in a low wavelength range (Figure 6b).

Figure 3

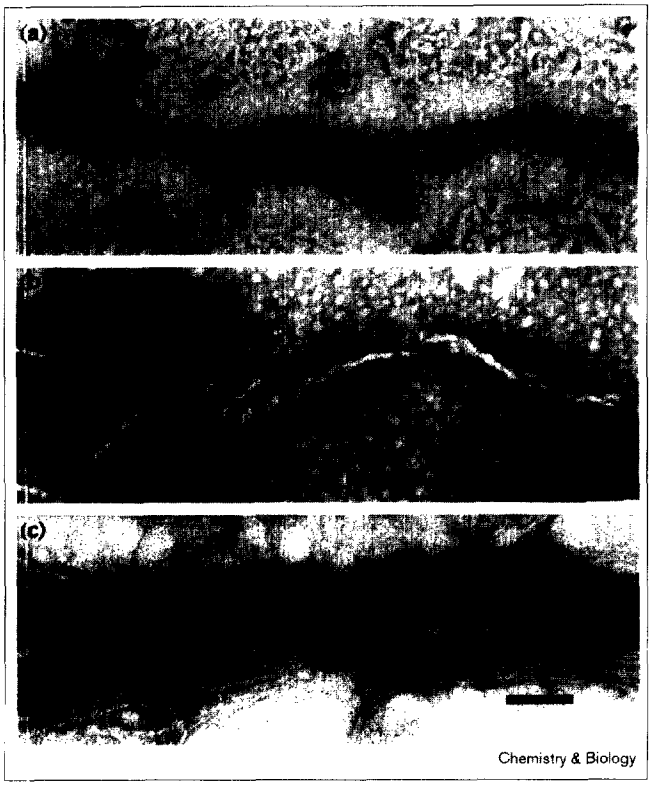

Electron microscopic examination of samples obtained after incubation. Aβ (80 μM) was dissolved and incubated in TBS, pH 7.4, for 40 min or 1 day and then centrifuged at 20,000 × g for 20 min. The resulting pellet was resuspended in water by brief sonication and 8 μl of this suspension was placed on a grid. Excess fluid was withdrawn after 30 s, the grid was negatively stained with 3% uranyl acetate in water, and examined in a JEOL EM 100CX. After 40 min of incubation, **(a)** a diffuse network of aggregated Aβ was observed, possibly representing a precursor of **(b)** the diffuse fibrils detected on the same grid. **(c)** After one day of incubation, only mature fibrils of Aβ, often packed in thick bundles, were detected. It is suggested that the diffuse fibrils in (b) are precursors of these mature fibrils. Scale bars, 100 nm.

Figure 4

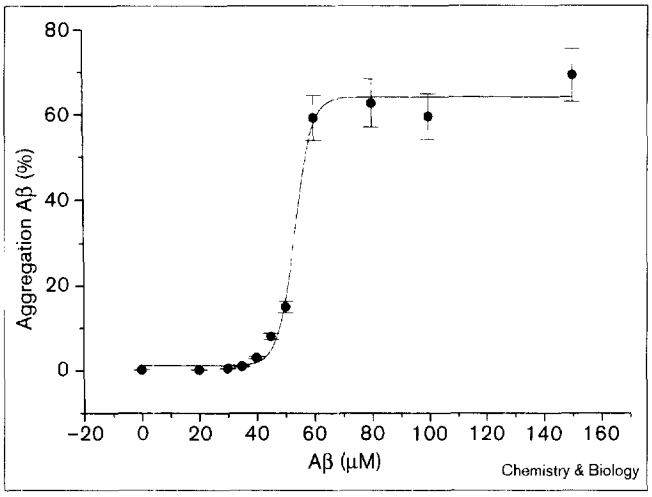

Aβ polymerization is strongly concentration dependent. Different concentrations of Aβ (20, 30, 35, 40, 45, 50, 60, 80, 100 and 150 μM) were incubated with 10 nM rhodamine-labeled Aβ. After a 40 min incubation, the percentage of Aβ aggregates was calculated as described in Figure 2.

Discussion

Previous studies have provided limited information on the early (1–120 min) phase of Aβ polymerization, largely due to problems in measuring monomers, oligomers and large aggregates simultaneously. We choose to study Aβ polymerization using FCS, as this technique is not limited in this way. In addition, measurements are made directly in solution without any further sample preparation, minimizing the risk for artefacts. Using FCS, we found that the polymerization of Aβ rapidly proceeds from monomers/dimers into large aggregates without significant amounts of free oligomer at any stage of the process. The absence of oligomers suggests that such intermediates are short-lived species in the initial phase of the aggregation process. It is possible that oligomers are formed within the large aggregates, however. These oligomers would not be detected with FCS because they would be 'trapped' in the aggregates. Very low concentrations of free oligomer (not bound to the large aggregates) could have escaped detection. To investigate their possible existence, cross-correlation spectroscopy could be used [49].

The aggregation of Aβ reached a maximum after 40 min, followed by a decrease towards a steady-state equilibrium after 2 h (Figure 2). From the diffusion time of the aggregates, the hydrodynamic radius was calculated to be ~60 μm. EM examination of samples incubated for 40 min revealed a network of amorphous structures and diffuse short fibrils. It is possible, therefore, that the large aggregates observed with FCS correspond to the amorphous networks seen in Figure 3a. The three-dimensional structure of such aggregates in solution is unclear, and, therefore, calculations that assumed shapes other than a sphere were not performed.

After incubation for 1 day, the diffusion time of the aggregates had decreased and corresponded to a hydrodynamic radius of ~6 μm. Only mature fibrils, often arranged as networks or in bundles with a diameter of about 100 nm, were observed with EM (Figure 3c). The diffusion time obtained by FCS was used to calculate the length of a rigid rod with a diameter of 100 nm. This length was found to be around 55 μm, somewhat larger than the lengths (about 5–20 μm) of the fibril bundles as estimated from EM. The possibility that the arrangement of the fibrils is altered during preparation for EM cannot be excluded, however. When samples incubated for 1 day were fixed with glutaraldehyde,

Figure 5

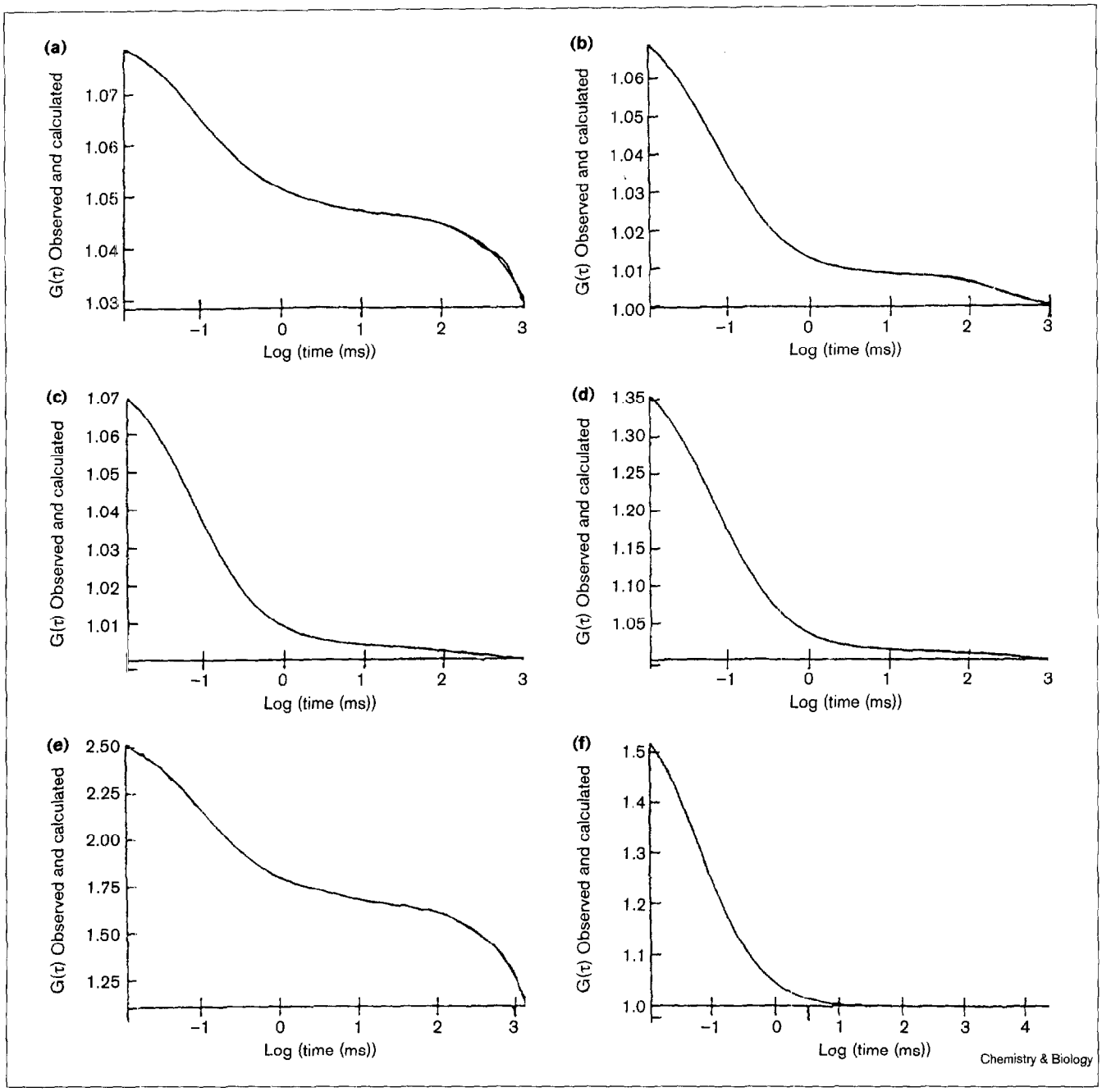

Dissolution of Aβ aggregates and displacement of rhodamine-labeled ligand with an excess of LBMP1620. Autocorrelation functions, G(τ) after incubation of Aβ (80 μM) and rhodamine-labeled Aβ (10 nM) for **(a)** 1 h **(b)** plus 2 h in the absence of or **(c)** in the presence of LBMP 1620 (320 μM). The proportion of large aggregates was found to be 20–25% and 5–6% after the additional 2 h of incubation without and with LBMP 1620, respectively. **(d)** If Aβ (80 μM) was dissolved in a solution containing LBMP 1620 (320 μM), only low amounts of aggregates (3–4%) were observed after 3 h of incubation. **(e)** The polymerization process can be followed with rhodamine-labeled ligand. Here, 100 μM Aβ was incubated for 1 h with 10 nM rhodamine-labeled ligand as a fluorescent probe. The autocorrelation function was apparently identical with that obtained using rhodamine-labeled Aβ, compare (a) with (e). **(f)** Rhodamine-labeled ligand could be completely displaced by incubating the solution in (e) with an excess of LBMP1620 (400 μM) for 2 h. The observed and calculated data points are completely overlapping.

embedded in plastic, sectioned and stained, spherical and ellipsoid fibril aggregates with diameters in the range of 1–5 μm were observed by EM (data not shown). The size of these aggregates is consistent with the diameter calculated

Figure 6

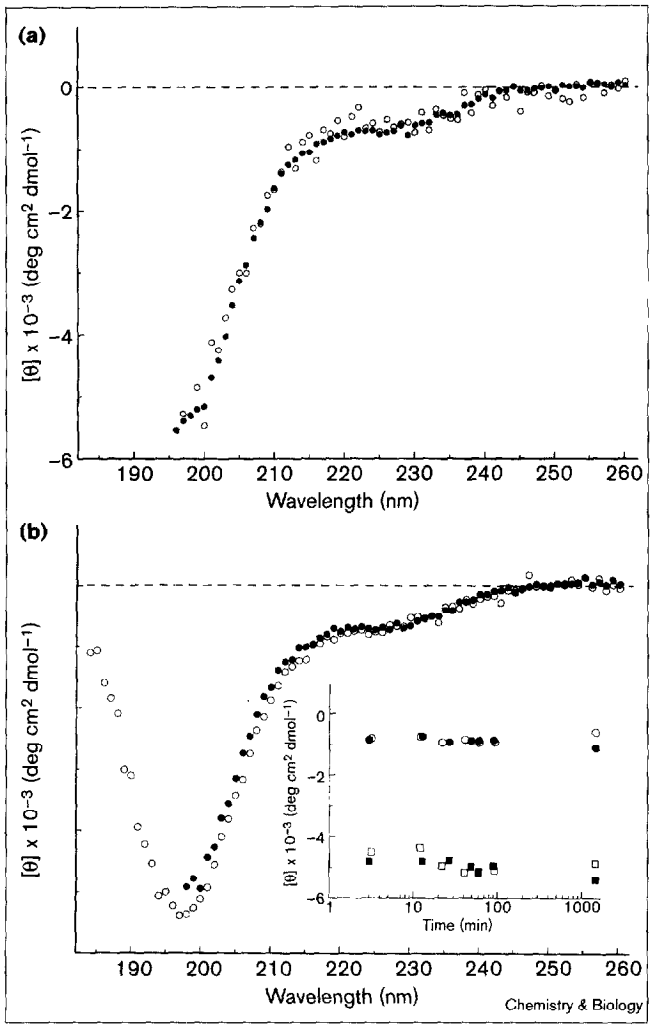

(a) CD spectra of $A\beta^{1-40}$ at 20 (open circles) and 80 μM (filled circles) 90 min after dissolution in TBS, pH 7.4. **(b)** Comparison of the spectra of $A\beta^{1-40}$, at 80 μM in TBS, pH 7.4 (filled circles) and 10 mM PO_4, 100 mM NaF, pH 7.4 (open circles) 90 min after dissolution. Time dependence of the CD signal in TBS, pH 7.4 (open symbols) and 10 mM PO_4, 100 mM NaF, pH 7.4 (filled symbols) at 217 (circles) and 200 nm (squares) is shown (inset).

from the diffusion times obtained with FCS. It is possible therefore that the fibrils are present in solution as more or less spherical aggregates.

Taken together, the data suggest that the formation of the large aggregates, possibly corresponding to the networks in Figure 3a, is one of the first important steps in Aβ fibril formation. The high local concentration of Aβ in these aggregates increases the probability of Aβ–Aβ interactions, followed by energetically favourable conformational changes and fibril growth. Eventually, these networks either dissolve into monomers/dimers (Figure 2b,c) or proceed into diffuse short fibrils (Figure 3b) and further into mature fibrils arranged in bundles (Figure 3c) or spherical aggregates. Findings similar to ours have recently been reported from electron spin resonance studies of the prion protein H1 peptide [50], in which it was also noticed that the fibrils were preceded by the formation of large amorphous aggregates, without any detectable amount of oligomers. The transient formation of very large aggregates could, therefore, be a general principle of amyloid assembly.

The early-stage aggregates observed using FCS have apparently escaped detection in previous light scattering and turbidimetric studies. Large aggregates of Aβ (with apparent molecular weights of 10^6 Da and 10^{10} Da) that might correspond to those observed using FCS and EM have previously been detected using analytical ultracentrifugation, however [20]. Analogous experiments on transthyretin also provide evidence for the existence of large soluble aggregates that do not scatter light [51]. Light-scattering methods are dependent on the refractive index of the species to be studied, so aggregates with a refractive index close to that of the aqueous buffer are not observed. FCS is not limited in this way. CD spectroscopy provides information about protein secondary structure and the time scale of the analysis is compatible with that of the early phase of Aβ polymerization. We could not detect any changes in secondary structure with CD spectroscopy within the first 24 h after dissolution of Aβ at 80 μM. The formation of the early large aggregates observed by FCS and EM was not revealed by CD analysis. Under the experimental conditions in which large aggregates of Aβ peptide were found by FCS (Figures 1,2), as well as the cooperative transition from monomers/dimers to large aggregates (Figure 4), no changes were observed in the CD spectra. The CD spectra were of random-coil type. We have found conditions at high peptide concentrations (150–300 μM) in which a transition to a typical β type CD spectrum similar to that reported by Seelig's group [31] was observed, and which might be connected to the formation of fibrillar structures. Given the behaviour of the CD spectra it is clear that the early larger aggregation phase is not connected to a change in the secondary structure of the Aβ peptide. The early larger aggregation phase can be envisaged as a transient stage preceding the fibril formation that might be linked to a concomitant β transition [31]. The finding that the Lys–Leu–Val–Phe–Phe peptide is able to dissolve the early Aβ aggregates more easily than the fibrillar forms could be connected to this behaviour.

The aggregation of Aβ was highly concentration dependent. No aggregates or oligomers were detected at concentrations below 50 μM Aβ and a sharp increase in aggregation occurred between 50–60 μM (Figure 4), which is in the range of the critical concentration (10–100 μM) reported by others [27,52–54]. The sharp phase transition observed (Figure 4) and the fact that practically no intermediate components in the aggregation process could be detected

by FCS indicate a highly cooperative interaction, as predicted by the seeding theory [55]. This theory postulates the formation of a short-lived multimeric aggregate, called a seed or a nucleus, to be the rate-limiting step. When a seed has formed, usually depicted as an aggregate of about eight monomers, the polymerization proceeds rapidly into fibrils. Our data indicates that the large diffuse networks are formed first; formation of oligomeric seeds could be facilitated within these networks. Using quasielastic light scattering, other investigators suggest that Aβ can form micelles in solutions at low pH. The micelles, formed at a critical concentration of ~100 μM, are either dissolved or transformed into seeds for fibril formation [27,53]. Although the aggregates we observe are much larger than micelles, they could represent clusters of micelles, each micelle being a possible seed for a fibril.

Incubation of Aβ in the presence of ligands, capable of binding to the Lys–Leu–Val–Phe–Phe motif, has been shown to inhibit fibril formation [18,19]. One of these ligands, LBMP 1620, was labeled and shown to bind both to monomeric/dimeric Aβ and aggregates of Aβ. Addition of an excess of LBMP1620 was shown to compete with labeled ligand, indicating a saturable and specific binding to Aβ. LBMP 1620 was found to decrease the amount, and to change the size distribution of the Aβ aggregates. The effect was most pronounced when the ligand was present from the start of the incubation. Interestingly, there was also a significant decrease in the amount of aggregates when the ligand was added after 1 h of incubation (Figure 5), indicating that the early large aggregates can be partly dissociated. The small populations of aggregates with diffusion times between 1 and 10 ms correspond to hydrodynamic radii of 3–35 nm. This is in the range of the size of protofibrils observed using atomic force microscopy [34,35], aggregates reported using quasielastic light scattering [27,28], and the diffuse fibrils reported here. The aggregates formed in the presence of ligand were found to be small and amorphous when examined using EM (data not shown), however, indicating that the species observed with FCS have structures less ordered than those of protofibrils or diffuse fibrils. Apparently, LBMP1620 acts in an early stage of the polymerization process by inhibiting the formation of the precursor of mature Aβ fibrils.

Significance

Accumulation of fibrillar deposits of Aβ in the brain is a crucial step in the pathogenesis of Alzheimer's disease. A detailed understanding of the molecular interactions of Aβ will facilitate the development of fibrillation inhibitors with potential to delay or prevent progression of the disease. Fluorescence correlation spectroscopy (FCS) provides fast and specific analysis of Aβ polymerization, with high sensitivity over a wide size distribution range. The polymerization proceeds from monomers/dimers to two populations of large aggregates, and fibrils are formed after a decline in the total amount of large aggregates, indicating a precursor–product relationship. Interfering with the formation of these large aggregates is therefore a potential strategy for inhibiting Aβ fibril formation. The effects of Aβ ligands can be studied with a fluorescently labeled ligand; FCS could therefore be used as a highly sensitive and specific competition assay to identify potential inhibitors of fibril formation. The appearance of Aβ aggregates in cerebrospinal fluid of Alzheimer's patients using FCS was reported recently and is suggested as a diagnostic tool [56].

Materials and methods

Materials

Rhodamine (tetramethylrhodamine-5-(and-6)-isothiocyanate) was purchased from Molecular Probes Europe BV, Leiden, The Netherlands. Synthetic $A\beta^{1-40}$ was obtained from David Teplow, the Biopolymer Laboratory at Harvard University. All other peptides (rhodamine-Lys-$A\beta^{1-40}$ (labeled only at the amino terminus in order to minimize the effects of the label), rhodamine-Lys–Lys–Leu–Val–Phe–Phe (labeled ligand), Lys–Lys–Leu–Val–Phe–Phe–Ala (LBMP1620), Lys–Leu–Val–Phe–Phe, Asn–Lys–Leu–Val–Phe–Phe–Ala, Lys–Ala–Leu–Val–Phe–Phe–Ala and the all D-amino acid peptide leu–phe–leu–arg–arg) were obtained from Research Genetics, Huntsville, AL, USA. Peptides were dissolved in 70% formic acid and purified on a polystyrene-divinylbenzene column (PLRP-S 150 × 25 mm, Polymer Laboratories, Church Stretton, UK) using a water-acetonitrile gradient with 0.1% trifluoroacetic acid. The peak fraction, peptide concentration ~30 μM in ~30% acetonitrile, was collected and immediately frozen. The purified peptides were lyophilized in the presence of dry ice (to avoid thawing and thus minimizing the risk of aggregation) and their identity and purity were checked using electrospray mass spectrometry. The mass spectrometer was a Quattro triple quadropol (Micromass, Altrincham, UK) fitted with an electrospray interface and spectra were recorded in the positive ion mode in the mass range 700–1700 m/z. Purity was also checked using HPLC using a C18 column (150 × 4.6 mm, Valco, USA). Purity was in all cases greater than 95%.

Fluorescence correlation spectroscopy instrumentation

FCS was performed with confocal illumination of a volume element of 0.23 femtolitres (fl) in an instrument as described previously [43]. As focusing optics a Zeiss Neofluar 63 × NA 1.2 was used in an epi-illumination setup. For separating excitation from emission radiation a dichroic filter (Omega 540 DRL PO^2) and a bandpass filter (Omega 565 DR 50) were used. Tetramethylrhodamine-labeled Aβ was excited with the 514.5 nm line of an Argon laser. The intensity fluctuations were detected by an avalanche photo-diode (EG & G SPCM 200) and were correlated with a digital correlator (ALV 5000, ALV, Langen, Germany). The ConfoCor instrument of Zeiss-Evotec (Jena, Germany), built according to the principles described previously [43], was used for the analysis as well. In this instrument a Neofluar 40 × NA 1.2 is used. The volume element in the ConfoCor was 0.19 fl.

FCS data evaluation

The intensity autocorrelation function G(τ) was analyzed according to a model describing the diffusion of a defined number of molecular species (two or three). For molecules diffusing in a finite three-dimensional Gaussian element [43] G(τ) is given by:

$$G(\tau) = 1 + \frac{1}{N}\sum_{i=1}^{2,3} \frac{x_i}{1+\frac{\tau}{\tau_{D_1}}} \sqrt{\frac{1}{1+\left(\frac{\omega}{z}\right)^2 \frac{\tau}{\tau_{D_i}}}} \qquad (1)$$

where N is the number of fluorescent molecules, x_i is the fraction of species i, with diffusion time τ_D, ω (0.5 μm) the radius and z (2 μm) the length of the volume element. The fraction of aggregation (F) was determined by:

$$F = \frac{x_2 + x_3}{x_1 + x_2 + x_3} \quad (2)$$

A more detailed analysis will have to take into account that x_i is also dependent on the number of labeled Aβ molecules incorporated, as well as on the quantum yield.

In order to assess the validity of the presence of discrete aggregates we analyzed G(τ) representing the distribution of diffusion times according to a model of multiple components:

$$G(\tau) = 1 + \frac{1}{N}\sum_{i=1}^{m} \frac{P_i}{1+\frac{\tau}{\tau_{Di}}} \sqrt{\frac{1}{1+\left(\frac{\omega}{z}\right)^2 \frac{\tau}{\tau_{Di}}}} \quad (3)$$

where P_i represents the distribution of diffusion time τ_D.

The diffusion time is related to the cross-section of the illuminated volume element and the diffusion constant D by:

$$\tau_D = \omega^2/4D \quad (4)$$

With the assumption that the studied species are spherical, the hydrodynamic radii, R_h, can be obtained from the Stoke–Einstein equation:

$$D = kT/(6\pi\eta R_h) \quad (5)$$

where η is the solvent viscosity, k is Boltzmann's constant and T is the absolute temperature. For the calculations we used T = 293 K and η = 1 cP (which corresponds to water).

For rod-like objects the translational diffusion constant D and rodlength L at given length/diameter, p = L/D, is obtained from [57]:

$$\frac{3\pi\eta LD}{kT} = \ln p + \gamma \quad (6)$$

Where γ = 0.38 is an end-effect correction at $p = \infty$ [57]. Substitution of Equations 4 and 6 yields

$$\tau_D = \frac{3\pi\eta\omega^2 L}{4kT(\ln p + \gamma)} \quad (7)$$

Thus, for a known diameter, for example, from EM of the fibril bundles, the corresponding length can be calculated from the diffusion time.

For parametrization and fitting of the autocorrelation function G(τ) nonlinear least squares minimization according to the Marquardt algorithm [58] was used. For evaluation of the distribution $P(\tau_{Di})$ the CONTIN algorithm [47,48] was applied.

FCS experiments

Free rhodamine was used to calibrate the instrument and as a reference to estimate the molecular weights of the dissolved peptides. The lyophilized peptides were dissolved directly in a buffer containing 50 mM Tris-HCl and 150 mM NaCl (TBS), pH 7.4, to concentrations ranging from 1 μM to 300 μM. The effect of Aβ ligands on polymerization was investigated by first dissolving the ligand in TBS and then adding the solution to lyophilized Aβ. The effect of ligands on preformed aggregates was studied by incubating a solution of 80 μM Aβ for 1 h and then dissolving the ligand in this solution. The ratio of Aβ : ligand ranged from 1:1 to 1:10. The labeled probe, rhodamine-Lys-Aβ or rhodamine-Lys–Lys–Leu–Val–Phe–Phe, was in all experiments added to the buffer before the unlabeled peptide was dissolved. The final concentration of labeled probe was 10 nM. Droplets (15 μl) of the samples were placed in a 8-well Nunc chamber (Nalge Nunc International, IL USA) covered with a lid, and analyzed for 30 s up to 10 min in the FCS instrument, at several time points of incubation, ranging from minutes to weeks. Both siliconized and non-siliconized sample chambers were used, without any detectable differences in results. All experiments were performed at 20°C.

Electron microscopy

The samples analyzed by FCS were centrifuged at 20,000 × g for 20 min, the supernatants were aspirated and the pellets were resuspended in 100 μl water by a brief sonication. In one set of experiments, the supernatants were aspirated without prior centrifugation. Aliquots (8 μl) of the resuspended material were placed on grids covered by a carbon-stabilized formvar film. After 30 s, excess fluid was withdrawn and the grids were negatively stained with 3% uranyl acetate in water. Finally, the specimens were examined and photographed in a JEOL EM 100CX instrument at 60 kV.

Quantification of supernatants using HPLC

Five μl of the samples were aspirated from the upper half of the solution. Prior to injection onto the HPLC column (Polymer Laboratories PLRP-S, 250 × 4.6 mm, 5 μm, 300 Å), 15 μl formic acid was added in order to dissolve aggregates of Aβ. The UV detector was set to 254 nm and the calculations were based on peak heights.

CD spectroscopy

Lyophilized $A\beta^{1-40}$ was dissolved in either: TBS, pH 7.4, 10 mM PO_4, 100 mM NaF, pH 7.4, or 5 mM MOPS, pH 7.4. CD spectra were recorded at 25.0°C in 0.1 cm cuvettes using an Aviv 62 DS spectropolarimeter (Aviv Assoc. Inc, Lakewood, NJ) between 260 and 180 nm with a spectral resolution of 1 nm and a spectral bandwidth of 1.5 nm. Data at time points < 20 min were recorded using an averaging time of 1 s/point (scan time < 160 s/spectrum), between 20 and 40 min, 8 s/point and at times > 40 min, 24 s/point. Raw CD data were converted to mean residue ellipticity, θ, in units of deg cm^2 $dmol^{-1}$.

Acknowledgements

The work was supported by the Swedish Medical Research Council (to J.T. and L.T.), the Swedish Heart Lung Foundation (to J.T.), the Swedish Natural Science Research Council (to R.R.), the Research Council for Engineering Sciences (to R.R.), The National Board of Health and Welfare (to S.B.) and the King Gustaf V 80th Birthday Fund (to J.T.). C.N. is a recipient of fellowships from the Swedish Medical Research Council, the Berth von Kantzow Foundation, the Swedish Society for Medical Research, the Axel Margret Axison Johnson Foundation and the Nicholson Foundation.

References

1. Glenner, G.G. & Wong, C.W. (1984). Alzheimer's disease: initial report of the purification and characterization of a novel cerebrovascular amyloid protein. *Biochem. Biophys. Res. Commun.* **120**, 885-890.
2. Masters, C.L., Simms, G., Weinman, N.A., Multhaup, G., McDonald, B.L. & Beyreuther, K. (1985). Amyloid plaque core protein in Alzheimer disease and Down syndrome. *Proc. Natl Acad. Sci. USA* **82**, 4245-4249.
3. Selkoe, D.J. (1994). Cell biology of the amyloid β-protein precursor and the mechanism of Alzheimer's disease. *Annu. Rev. Cell. Biol.* **10**, 373-403.
4. Goate, A., *et al.*, & Hardy, J. (1991). Segregation of a missense mutation in the amyloid precursor protein gene with familial Alzheimer's disease. *Nature* **349**, 704-706.
5. Mullan, M., *et al.*, & Crawford, F. (1992). A pathogenic mutation for probable Alzheimer's disease in the APP gene at the amino terminus of β-amyloid. *Nat. Genet.* **1**, 345-347.
6. Sherrington, R., *et al.*, & St George-Hyslop, P.H. (1995). Cloning of a gene bearing missense mutations in early-onset familial Alzheimer's disease. *Nature* **375**, 754-760.
7. Rogaev, E.I., *et al.*, & St George-Hyslop, P.H. (1995). Familial Alzheimer's disease in kindreds with missense mutations in a gene on chromosome 1 related to the Alzheimer's disease type 3 gene. *Nature* **376**, 775-778.

8. Levy-Lahad, E., *et al.*, & Schellenberg, G.D. (1995). A familial Alzheimer's disease locus on chromosome 1. *Science* **269**, 970-973.
9. Scheuner, D., *et al.*, & Younkin, S. (1996). Secreted amyloid beta-protein similar to that in the senile plaques of Alzheimer's disease is increased *in vivo* by the presenilin 1 and 2 and APP mutations linked to familial Alzheimer's disease. *Nat. Med.* **2**, 864-870.
10. Games, D., *et al.*, & Zhao, J. (1995). Alzheimer-type neuropathology in transgenic mice overexpressing V717F β-amyloid precursor protein. *Nature* **373**, 523-527.
11. Hsiao, K., *et al.*, & Cole, G. (1996). Correlative memory deficits, Aβ elevation, and amyloid plaques in transgenic mice. *Science* **274**, 99-102.
12. Pike, C.J., Burdick, D., Walencewicz, A.J., Glabe, C.G. & Cotman, C.W. (1993). Neurodegeneration induced by β-amyloid peptides *in vitro*: the role of peptide assembly state. *J. Neurosci.* **13**, 1676-1687.
13. Lorenzo, A. & Yankner, B.A. (1994). β-amyloid neurotoxicity requires fibril formation and is inhibited by Congo red. *Proc. Natl Acad. Sci. USA* **91**, 12243-12247.
14. Iversen, L.L., Mortishire-Smith, R.J., Pollack, S.J. & Shearman, M.S. (1995). The toxicity in vitro of β-amyloid protein. *Biochem. J.* **311**, 1-16.
15. Camilleri, P., Haskins, N.J. & Howlett, D.R. (1994). β-Cyclodextrin interacts with the Alzheimer amyloid β-A4 peptide. *FEBS Lett.* **341**, 256-258.
16. Tomiyama, T., *et al.*, & Endo, N. (1996). Inhibition of amyloid β protein aggregation and neurotoxicity by rifampicin. *J. Biol. Chem.* **1996**, 6839-6844.
17. Ghanta, J., Shen, C.-H., Kiessling, L.L. & Murphy, R.M. (1996). A strategy for designing inhibitors of β-amyloid toxicity. *J. Biol. Chem.* **271**, 29525-29528.
18. Tjernberg, L.O., *et al.*, & Nordstedt, C. (1996). Arrest of β-amyloid fibril formation by a pentapeptide ligand. *J. Biol. Chem.* **271**, 8545-8548.
19. Tjernberg, L.O., *et al.*, & Nordstedt, C. (1997). Controlling amyloid β-peptide fibril formation with protease-stable ligands. *J. Biol. Chem.* **272**, 12601-12605.
20. Snyder, S.W., *et al.*, & Holzman, T.F. (1994). Amyloid-β aggregation: selective inhibition of aggregation in mixtures of amyloid with different chain lengths. *Biophys. J.* **67**, 1216-1228.
21. Tomiyama, T., Asano, S., Furiya, Y., Shirasawa, T., Endo, N. & Mori, H. (1994). Racemization of Asp23 residue affects the aggregation properties of Alzheimer amyloid β protein analogues. *J. Biol. Chem.* **269**, 10205-10208.
22. Soto, C., Castano, E.M., Frangione, B. & Inestrosa, N.C. (1995). The α-helical to β-strand transition in the amino-terminal fragment of the amyloid β-peptide modulates amyloid formation. *J. Biol. Chem.* **270**, 3063-3067.
23. Wood, S.J., Maleeff, B., Hart, T. & Wetzel, R. (1996). Physical, morphological and functional differences between pH 5.8 and 7.4 aggregates of the Alzheimer's amyloid peptide Aβ. *J. Mol. Biol.* **256**, 870-877.
24. Shen, C.L., Scott, G.L., Merchant, F. & Murphy, R.M. (1993). Light scattering analysis of fibril growth from the amino-terminal fragment β(1–28) of β-amyloid peptide. *Biophys. J.* **65**, 2383-2395.
25. Shen, C.L., Fitzgerald, M.C. & Murphy, R.M. (1994). Effect of acid predissolution on fibril size and fibril flexibility of synthetic β-amyloid peptide. *Biophys. J.* **67**, 1238-1246.
26. Shen, C.-H. & Murphy, R.M. (1995). Solvent effects on self-assembly of β–amyloid peptide. *Biophys. J.* **69**, 640-651.
27. Lomakin, A., Chung, D.S., Benedek, G.B., Kirschner, D.A. & Teplow, D.B. (1996). On the nucleation and growth of amyloid β-protein fibrils: detection of nuclei and quantitation of rate constants. *Proc. Natl Acad. Sci. USA* **93**, 1125-1129.
28. Walsh, D.M., Lomakin, A., Benedek, G.B., Condron, M.M. & Teplow, D.B. (1997). Amyloid β-protein fibrillogenesis. *J. Biol. Chem.* **272**, 22364-22372.
29. Hilbich, C., Kisters-Woike, B., Reed, J., Masters, C.L. & Beyreuther, K. (1991). Aggregation and secondary structure of synthetic amyloid βA4 peptides of Alzheimer's disease. *J. Mol. Biol.* **218**, 149-163.
30. Barrow, C.J., Yasuda, A., Kenny, P.T. & Zagorski, M.G. (1992). Solution conformations and aggregational properties of synthetic amyloid β-peptides of Alzheimer's disease. Analysis of circular dichroism spectra. *J. Mol. Biol.* **225**, 1075-1093.
31. Terzi, E., Hölzemann, G. & Seelig, J. (1995). Self-association of β-amyloid peptide (1-40) in solution and binding to lipid membranes. *J. Mol. Biol.* **252**, 633-642.
32. Naiki, H. & Nakakuki, K. (1996). First-order kinetic model of Alzheimer's β-amyloid fibril extension *in vivo*. *Lab. Invest.* **74**, 374-383.
33. Stine W.B.Jr., *et al.*, & Krafft, G.A. (1996). The nanometer-scale structure of amyloid-β visualized by atomic force microscopy. *J. Protein Chem.* **15**, 193-203.
34. Harper, J.D., Wong, S., Lieber, C.M. & Lansbury, P.T., Jr. (1997). Observation of metastable Aβ amyloid protofibrils by atomic force microscopy. *Chem. Biol.* **4**, 119-125.
35. Harper, J.D., Lieber, C.M. & Lansbury, P.T., Jr. (1997). Atomic force microscopic imaging of seeded fibril formation and fibril branching by the Alzheimer's disease amyloid-β protein. *Chem. Biol.* **4**, 951-959.
36. Burdick, D., *et al.*, & Glabe, C. (1992). Assembly and aggregation properties of synthetic Alzheimer's A4/β amyloid peptide analogs. *J. Biol. Chem.* **267**, 546-554.
37. Sweeney, P.J., Darker, J.G., Neville, W.A., Humphries, J. & Camilleri, P. (1993). Electrophoretic techniques for the analysis of synthetic amyloid β-A4-related peptides. *Anal. Biochem.* **212**, 179-184.
38. Garzon-Rodriguez, W., Sepulveda-Becerra, M., Milton, S. & Glabe, C.G. (1997). Soluble amyloid Aβ-(1–40) exists as a stable dimer at low concentrations. *J. Biol. Chem.* **272**, 21037-21044.
39. LeVine, H., III. (1993). Thioflavine T interaction with synthetic Alzheimer's disease β-amyloid peptides: detection of amyloid aggregation in solution. *Protein Sci.* **2**, 404-410.
40. Magde, D., Elson, E.L. & Webb, W.W. (1972). Thermodynamic fluctuations in a reacting system. Measurement by fluorescence correlation spectroscopy. *Phys. Rev. Lett.* **29**, 705-711.
41. Elson, E.L. & Magde, D. (1974). Fluorescence correlation spectroscopy. I. Conceptual basis and theory. *Biopolymers* **13**, 1-27.
42. Ehrenberg, M. & Rigler, R. (1974). Rotational Brownian motion and fluorescence intensity fluctuation. *Chem. Phys.* **4**, 390-401.
43. Rigler, R., Mets, Ü., Widengren, J. & Kask, P. (1993). Fluorescence correlation spectroscopy with high count rate and low background: Analysis of translational diffusion. *Eur. Biophys. J.* **22**, 169-175.
44. Eigen, M. & Rigler, R. (1994). Sorting single molecules: application to diagnostics and evolutionary biotechnology. *Proc. Natl Acad. Sci. USA* **91**, 5740-5747.
45. Rigler, R. (1995). Fluorescence correlations, single molecule detection and large number screening. Applications in biotechnology. *J. Biotech.* **41**, 177-186.
46. Tjernberg, L. (1997). Molecular basis and pharmacological implications of Alzheimer amyloid β-peptide fibril formation [PhD thesis]. Karolinska Institute, Stockholm, Sweden.
47. Provencher, S.W. (1982). A constrained regulation method for inverting data represented by linear algebraic or integral equations. *Computer Physics Commun.* **27**, 213-227.
48. Provencher, S.W. (1982). Contin: a general purpose constrained regulation program for inverting noisy linear algebraic and integral equations. *Computer Physics Commun.* **27**, 229-242.
49. Schwille, P., Meyer-Almes, F.J. & Rigler, R. (1997). Dual-color fluorescence cross-correlation spectroscopy for multicomponent diffusional analysis in solution. *Biophys. J.* **72**, 1878-1886.
50. Lundberg, K.M., Stenland C.J., Cohen, F.E., Prusiner, S.B. & Millhauser, G.L. (1997). Kinetics and mechanism of amyloid formation by the prion protein H1 peptide as determined by time-dependent ESR. *Chem. Biol.* **4**, 345-355.
51. Kelly, J.W. (1996). Fibril structure. General discussion I. *Ciba Foundation Symposium* **199**, p. 43, Wiley & Sons, Chichester, UK.
52. Soreghan, B., Kosmoski, J. & Glabe, C. (1994). Surfactant properties of Alzheimer's Aβ peptides and the mechanism of amyloid aggregation. *J. Biol. Chem.* **269**, 28551-28554.
53. Jarrett, J.T., Berger, E.P. & Lansbury, P.T., Jr. (1993). The carboxyl terminus of the β amyloid protein is critical for the seeding of amyloid formation: implications for the pathogenesis of Alzheimer's disease. *Biochemistry* **32**, 4693-4697.
54. Evans, K.C., Berger, E.P., Cho, C.G., Weisgraber, K.H. & Lansbury, P.T., Jr. (1995). Apolipoprotein E is a kinetic but not a thermodynamic inhibitor of amyloid formation: implications for the pathogenesis and treatment of Alzheimer's disease. *Proc. Natl Acad. Sci. USA* **92**, 763-767.
55. Jarrett, J.T. & Lansbury, P.T., Jr. (1993). Seeding 'one-dimensional crystallization' of amyloid: a pathogenic mechanism in Alzheimer's disease and scrapie? *Cell* **73**, 1055-1058.
56. Pitschke, M., Prior, R., Haupt, M. & Riesner, D. (1998). Detection of single amyloid β-protein aggregates in the cerebrospinal fluid of Alzheimer's patients by fluorescence correlation spectroscopy. *Nat. Med.* **4**, 832-834.
57. de la Torre, J.G. & Bloomfield, V.A. (1981). Hydrodynamic properties of complex, rigid, biological macromolecules: theory and applications. *Q. Rev. Biophys.* **14**, 81-139.
58. Marquardt, D.W. (1963). An algorithm for least-squares estimation of nonlinear parameters. *J. Soc. Indust. Appl. Math.* **11**, 431-441.